Engineering 1D Quantum Stripes from Superlattices of 2D Layered Materials

John H. Gruenewald, Jungho Kim, Heung Sik Kim, Jared M. Johnson, Jinwoo Hwang, Maryam Souri, Jasminka Terzic, Seo Hyoung Chang, Ayman Said, Joseph W. Brill, Gang Cao, Hae-Young Kee, and Sung S. Ambrose Seo*

An ideal 1D quantum-stripe consists of an infinite linear chain of bonded atoms, wherein the interactions between each atom's electrons are restricted to the single dimension of the chain.[1] 1D order spontaneously emerges at the onset of quantum phase transitions in the form of charge/spin density waves in multiferroics, superconductors, and as edge and surface states in topologically nontrivial systems.[2–8] An experimental approach for investigating such phenomena is to dimensionally tune these systems to 1D until a critical phase transition is reached, as conducted similarly in Ruddlesden–Popper series compounds from three to two dimensions.[9] While many successful strategies have been demonstrated for chemically synthesizing 1D nanostructures, direct atomic-layer control between two and one dimension(s) is generally considered unavailable.[10] Additionally, the quantum confinement of conventionally 2D materials to 1D can reveal hidden electronic and magnetic properties. For example, $SrCuO_2$, i.e., 1D chain compound, shows novel spin-charge separation, which is absent in its 2D counterpart, $Sr_2CuO_2Cl_2$ (Kim et al.[11]). Despite the promising outlook for 1D materials, experimental progress remains in its infancy, hampered by its reliance on the few materials with intrinsic 1D structures.[12]

Here, we present a new approach of synthesizing 1D quantum systems by constructing dimensionally confined stripe-superlattices from *in-plane* oriented 2D layered crystals.

J. H. Gruenewald, M. Souri, J. Terzic, Prof. J. W. Brill,
Prof. G. Cao, Prof. S. S. A. Seo
Department of Physics and Astronomy
University of Kentucky
Lexington, KY 40506, USA
E-mail: a.seo@uky.edu
Dr. J. Kim, Dr. A. Said
Advanced Photon Source
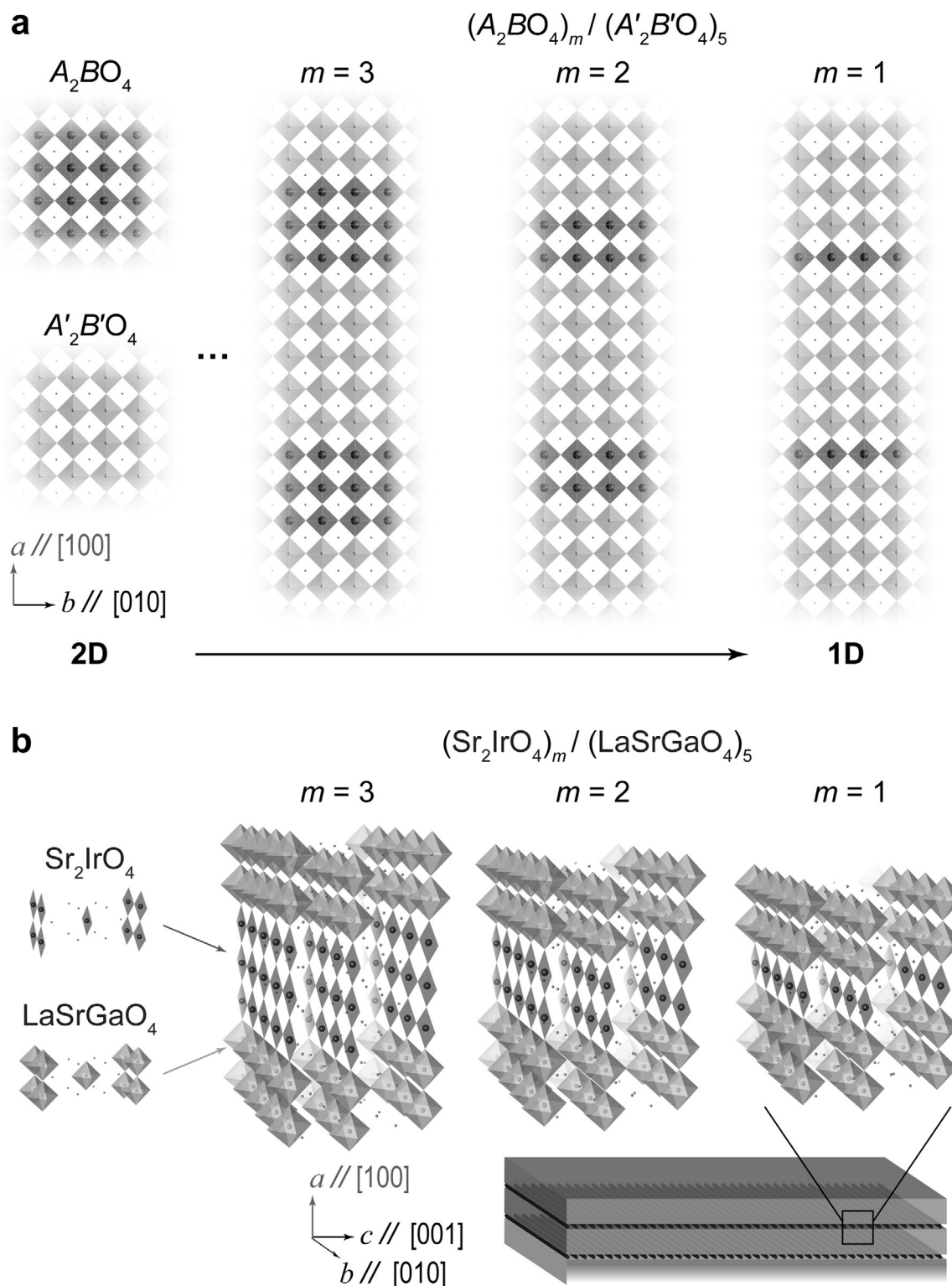Argonne National Laboratory
Argonne, IL 60439, USA
Dr. H. S. Kim, Prof. H. Y. Kee
Department of Physics
University of Toronto
Toronto, Ontario M5S 1A7, Canada
J. M. Johnson, Prof. J. Hwang
Department of Materials Science and Engineering
The Ohio State University
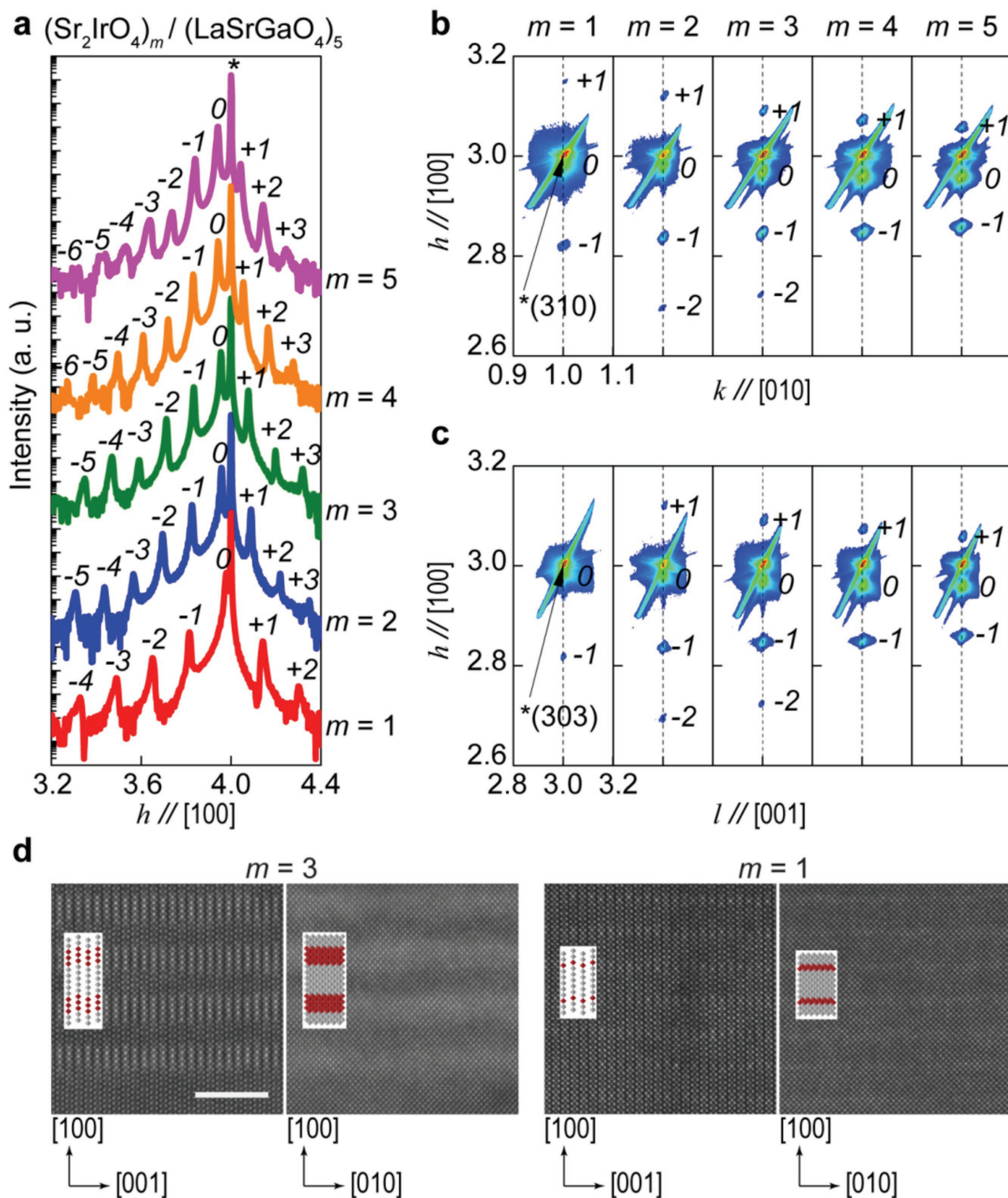Columbus, OH 43210, USA
Dr. S. H. Chang
Materials Science Division
Argonne National Laboratory
Argonne, IL 60439, USA

Layered transition metal oxides of the form A_2BO_4 consist of 2D layers (BO_2) in the *ab*-plane that are stacked along the *c*-axis. Such materials are considered 2D, since each consecutive plane is well separated by an electronically inert rock salt layer (*AO*) and offset by a half unit cell. Compounds with this so-termed K_2NiF_4-type structure can be epitaxially grown such that the 2D layers are oriented parallel to the surface normal direction, i.e., *a*-axis orientation.[13–15] The crux of our idea is that the dimensionality of the 2D layered materials in this *a*-axis orientation can be tuned by restricting the number of monolayers *m* grown along the *in*-plane direction (**Figure 1**a). For instance, if only a single monolayer is grown, i.e., $m = 1$, then the 2D planes become 1D stripes. To achieve a volume suitable for experimental characterizations, superlattice structures can be grown consisting of alternating layers of *m* monolayers of BO_2 and *n* monolayers of an inert, wide bandgap material also containing the K_2NiF_4 symmetry ($A'_2B'O_4$). In this manner, the 2D planes can be incrementally tuned to 1D quantum stripes.

We have implemented this idea in synthesizing 1D IrO_2 stripes using in-plane oriented superlattices of Sr_2IrO_4 and the wide-bandgap insulator $LaSrGaO_4$ ($E_g = 3.8$ eV) (Figure 1b and Figure S1 in the Supporting Information). The 2D layered iridate Sr_2IrO_4 exhibits a unique spin-orbit coupled $J_{eff} = 1/2$ Mott insulating state, which is not present in its 3D metallic counterpart $SrIrO_3$.[16–19] Recent studies on 2D Sr_2IrO_4 also have revealed interesting phenomena such as the presence of excitonic quasiparticles and indications of new superconducting ground states for doped samples.[20–23] Although expected to form intriguing electronic and magnetic ground states in one dimension, there are no previously studied or discovered 1D iridate systems to date. To synthesize the 1D superlattice structures, we have used a customized pulsed laser deposition system in order to optimize monolayer-controlled deposition of Sr_2IrO_4 and $LaSrGaO_4$ (see the Supporting Information and ref. [24] for detailed growth methods and conditions). Using structural and electronic characterizations of X-ray diffraction, high-resolution scanning transmission electron microscopy (STEM), optical spectroscopy, and resonant inelastic X-ray scattering, we have confirmed that both 1D structural and electronic confinement is achieved for this system. Our experimental observations are also consistent with the calculations of density functional theory. These results imply that this method can be extended to any 2D layered material and thereby allow for tunability to 1D quantum structures previously disregarded in experimental 1D science.

The 1D stripe-structures of our superlattice samples have been confirmed by X-ray diffraction and high-resolution STEM. **Figure 2**a shows clear periodic superlattice peaks in the 2θ–ω

Figure 1. Conceptual diagram of turning a 2D layered material into a 1D quantum stripe superlattice. a) The leftmost panel shows the in-plane structures of two transition-metal oxides, A_2BO_4 (above) and $A'_2B'O_4$ (below), with the K_2NiF_4 symmetry. Each dark gray (light gray) square contains transition-metal ions B (B') at its center and an oxygen atom at each of its four vertices. The number of BO_2 monolayers m corresponds to the horizontal rows of dark gray squares, i.e., the stripes. Low-dimensional stripe phases approaching 1D (e.g., $m = 3, 2, 1$) can be created by alternating the layers between m monolayers of BO_2 and a constant number of $B'O_2$ monolayers (such as 5 in the schematic). The 1D quantum stripes are achieved in the $m = 1$ case depicted in the rightmost panel. b) Schematic diagrams of a-axis-oriented $(Sr_2IrO_4)_m/(LaSrGaO_4)_5$ superlattices for $m = 3$, $m = 2$, and $m = 1$ for realizing the low-dimensional quantum stripes of IrO_2 (dark gray squares) on $LaSrGaO_4$ (100) substrates. The 1D IrO_2 stripes run parallel to the b-axis and are dimensionally confined by the wide-bandgap $LaSrGaO_4$ layers (light grey octahedra).

ADVANCED
SCIENCE NEWS
www.advancedsciencenews.com

ADVANCED
MATERIALS
www.advmat.de

COMMUNICATION

Figure 2. X-ray diffraction scans and Z-contrast STEM data of $(Sr_2IrO_4)_m/(LaSrGaO_4)_5$ superlattices. a) 2θ–ω X-ray diffraction scans of $(Sr_2IrO_4)_m/$ $(LaSrGaO_4)_5$ superlattices (labeled accordingly to the right). The LaSrGaO$_4$ (400)-diffraction peaks are indicated by an asterisk (*). The central super-lattice peak is the zeroth-order Bragg diffraction peak (indexed as 0), and the superlattice satellite peaks are indexed relative to this peak. b,c) Two X-ray reciprocal space maps are taken for each superlattice sample about the (310) reflection (b) and the (303) reflection (c) of LaSrGaO$_4$ (*) to obtain complete in-plane strain information. d) Z-contrast STEM images of $m = 3$ (left pair) and $m = 1$ (right pair) superlattices. Two cross-sections are shown for each sample: the ac-plane (left scan of each pair) and the ab-plane (right scan of each pair). The brightest dots are Ir ions and the inset schematics employ the same color scheme as in Figure 1b. Note that the IrO$_2$ stripes run along the b-axis ([010]-direction), that is the out-of-page direction in the left image and the horizontal direction in the right image of each sample. All the images have the same scale bar (leftmost image) of 5 nm.

X-ray diffraction scans. Since each superlattice unit cell consists of m monolayers of Sr_2IrO_4 and five monolayers of $LaSrGaO_4$, i.e., $(Sr_2IrO_4)_m/(LaSrGaO_4)_5$ ($m = 1$–5), the superlattice diffraction peak periodicity Δh shows excellent agreement to $1/(m + 5)$. For strain information, X-ray reciprocal space maps have been taken near the (310) and (303) reflections of $LaSrGaO_4$ for the ab- (Figure 2b) and ac-planes (Figure 2c), respectively. The vertical alignment of the superlattice peaks with the substrate reflections indicates all superlattices are coherently strained along both directions, i.e., b- and c-axes. STEM further confirms that the 1D superlattice structures are successfully formed (Figure 2d). The expected half-unit cell offset (zig-zag shape) and Sr–O rock salt separation between neighboring IrO_2 stripes along the c-axis is readily apparent in the ac-plane scans of the $m = 3$ and $m = 1$ samples. Along the b-axis, the IrO_2 stripes are coherent; however, the stripe boundaries in this planar view are rather indeterminate due to the interstripe half-unit-cell offset between each planar layer. These observations provide convincing evidence for the successful creation of 1D IrO_2 stripe-structures from the 2D Sr_2IrO_4.
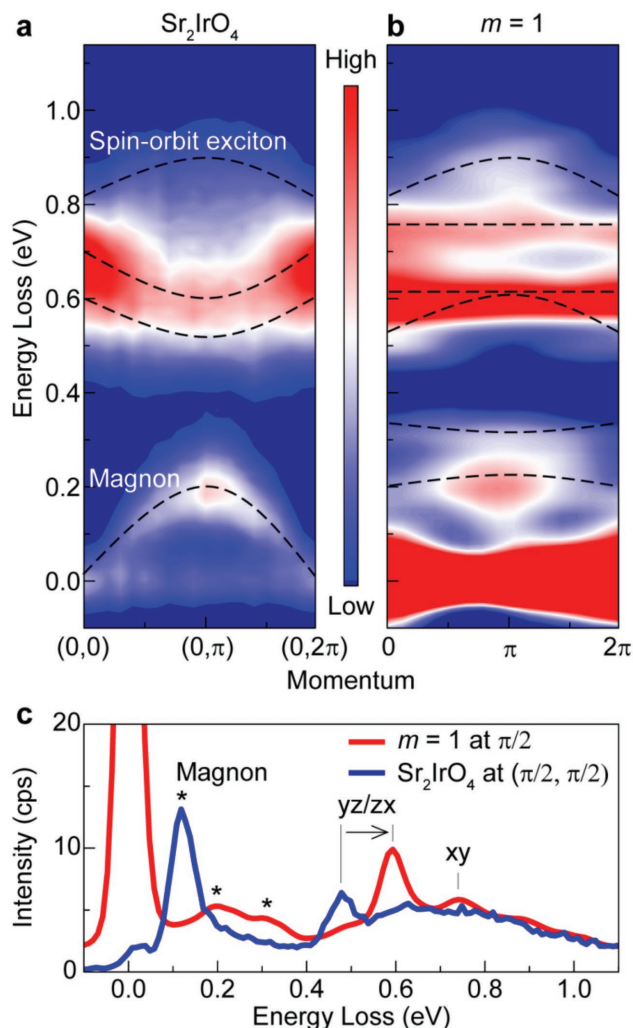
Linearly polarized optical spectroscopy shows clear anisotropic characteristics and 1D electronic confinement of the stripe-structures. The directional-dependent absorption spectra are obtained by linearly polarizing the incident photons such that the electric field E is perpendicular (parallel) to the 1D IrO_2 stripe direction along the b-axis, as shown by the graphic in **Figure 3**a (Figure 3b). The optical conductivity spectra ($\sigma_1(\omega)$) are obtained by taking a Kramers–Kronig transformation of the absorption spectra $\alpha(\omega)$ (Figure S4 in the Supporting Information) and are normalized by the number of Ir monolayers per superlattice unit cell, i.e., $m/(m + 5)$ for the $(Sr_2IrO_4)_m/(LaSrGaO_4)_5$ superlattices. When the polarization is parallel to the 1D IrO_2 stripe direction, i.e., $E//b$ (Figure 3b), there are broad peaks in the optical spectra. The finite peaks appear due to the Ir–Ir intersite optical transitions in the $J_{eff} = 1/2$ band.[21,25,26] Note that the peaks are significantly reduced (Figure 3a) when the polarization is perpendicular to the IrO_2 stripe direction, i.e., $E \perp b$. If the IrO_2 stripes are truly 1D, this can be understood intuitively since no Ir–Ir intersite optical transitions are possible perpendicular to the b-axis. Hence, the observation of optical anisotropy confirms that the 1D IrO_2 stripes are also confined electronically. As m decreases, i.e., the samples approach one dimension, the spectral weight in the absorption is reduced (Figure S4 in the Supporting Information) and the indirect gap observed in 2D Sr_2IrO_4 (Figure 3c) becomes a direct gap for the 1D superlattices (Figure 3d). New sharp features also appear in the spectra (marked as ∇ in Figure 3b). The sharp features present in the optical spectra are attributed to van Hove singularities, the appearance of which is contingent upon the low dimensionality of the crystal.[27] The low dimensionality also contributes to an enhanced effective electron correlation U_{eff}, which is responsible for the blueshift of the optical transitions (Figure S4 in the Supporting Information).

In order to reveal the elementary excitation dynamics of spin/orbital degrees of freedom exhibited by the 1D IrO_2 stripe-structures, we have taken resonant inelastic X-ray scattering (RIXS) spectra (For measurement geometry, see Figure S6 in the Supporting Information). In the case of 2D Sr_2IrO_4,
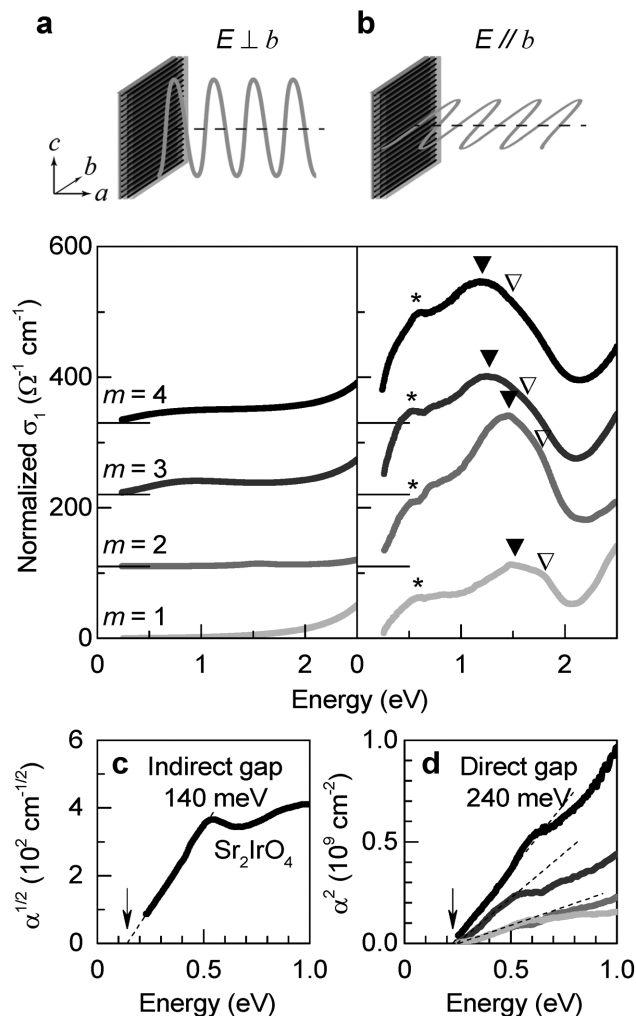
Figure 3. a,b) Optical spectra of $(Sr_2IrO_4)_m/(LaSrGaO_4)_5$ superlattices. Above each plot, an experimental depiction of the two sets of incident photons with linear polarization (E) perpendicular (a) and parallel (b) to the IrO_2 stripe-direction (b-axis) for $m = 1$ (light gray), 2 (gray), 3 (dark gray), and 4 (black) superlattices. All the optical conductivity spectra σ_1 are normalized by the number of Ir monolayers per superlattice unit cell for comparison, and $m = 2$, 3, and 4 spectra are vertically shifted for clarity. The strong optical anisotropy, i.e., the absence of the low-energy absorption peaks when E is perpendicular to the 1D IrO_2 stripes, confirms the low-dimensional electronic confinement. In the $m = 4$ superlattice spectra, the two peaks indicated by * and ▼ closely match the peak positions of 2D Sr_2IrO_4 crystals.[15] c,d) As the dimensionality decreases, several notable features include: the change in electronic band and optical gap nature from an indirect gap (c) (band edge linear with $\alpha^{1/2}$) to a direct gap (d) (band edge linear with α^2), the appearance of van Hove singularities, the distinct emergence of a higher energy peak marked by ∇, and a blue-shift of the ▼ peak.

RIXS spectra reveal a magnon produced by antiferromagnetic Heisenberg spin below 0.2 eV as well as dispersive excitonic quasiparticles of J_{eff} orbitals (spin-orbit excitons) above 0.4 eV (**Figure 4**a and Kim et al.[20]). For the 1D superlattice, the $m = 1$ RIXS spectra reveal many unique features not present in its 2D Sr_2IrO_4 counterpart (Figure 4b and Figure 4c). The spin excitation energy of the 1D IrO_2 stripes ($\approx$0.2 eV) is higher than that of 2D Sr_2IrO_4 ($\approx$0.06 eV), which implies that the 1D IrO_2 stripes

**ADVANCED
SCIENCE NEWS**
www.advancedsciencenews.com

**ADVANCED
MATERIALS**
www.advmat.de

COMMUNICATION

Figure 4. a,b) Intensity contour plots of RIXS spectra for 2D Sr_2IrO_4 crystal along the (0,0) to (0,2π) direction of its 2D Brillouin zone (a) and 1D $(Sr_2IrO_4)_1/(LaSrGaO_4)_5$ superlattice along the 0 to 2π direction (i.e., parallel to the b-axis) of its 1D Brillouin zone (b). Note that the low-energy magnon branch and the dispersion of spin-orbit excitons are shown below 0.2 eV and above 0.4 eV, respectively, and dashed lines act as visual guides for qualitatively contrasting the dimensionality effect on these dispersive features. c) RIXS spectra of 1D $(Sr_2IrO_4)_1/(LaSrGaO_4)_5$ superlattice (red) and 2D Sr_2IrO_4 crystal (blue) at comparable momentum transfers, i.e., $\pi/2$ and ($\pi/2$, $\pi/2$), respectively. Distinct excitations of the 1D superlattice include the following: broad spin-excitations of the 1D superlattice below 0.4 eV are in sharp contrast from the resolution-limited magnon peak of 2D Sr_2IrO_4 (indicated by * in (c)); the 1D superlattice shows a quasiparticle spin-orbit exciton at $\approx$0.6 eV, of which energy is 100 meV higher than that of 2D Sr_2IrO_4; and broad orbital excitations also show different dispersive behaviors from 2D counterpart. The strong intensity around zero energy loss in the 1D superlattice spectra is mostly from elastic scattering by $LaSrGaO_4$ layers.

have higher exchange interactions due to the localized character of the 1D spin structure. In the region of orbital excitations, a resolution-limited spin-orbit exciton at 0.6 eV is discovered. This is interpreted as arising from the same J_{eff} orbital transitions of the spin-orbit exciton in bulk Sr_2IrO_4—with a notable exception of broad dispersive excitations within the vicinity

of the 1D spin-orbit exciton. These broad excitations disperse toward higher energy as the momentum transfer approaches π (Figure 4b). Note that broad excitations in bulk Sr_2IrO_4 originate from the electron–hole continuum and damped orbital excitons. Thus, the broad dispersive excitations in the 1D IrO_2 stripe RIXS spectra are consistent with the optical spectroscopy data (Figure 3b), which reveal the existence of a largely reduced electron–hole continuum. Hence, the observed broad orbital excitations reflect the deconfined character of orbitals in the 1D structure.

To supplement the understanding of the experimental data, we have performed density functional theory calculations for the 1D $(Sr_2IrO_4)_1/(LaSrGaO_4)_5$ stripe-structure. As compared to its 2D Sr_2IrO_4 counterpart (Figure S5a in the Supporting Information), the spin-orbit split $J_{eff} = 1/2$ band appears quite flattened in the 1D energy dispersion (Figure S5b in the Supporting Information), indicating the presence of a very localized $J_{eff} = 1/2$ state. As a consequence, the indirect gap between the $J_{eff} = 1/2$ state in 2D Sr_2IrO_4 becomes a direct gap in its 1D counterpart, which is in excellent agreement with the indirect-to-direct gap phase transition observed in the optical spectra (Figures 3c,d, respectively). The localization of the $J_{eff} = 1/2$ state should also induce additional sharp optical transitions, since optical spectroscopy measures the joint density of states between occupied and unoccupied bands. This result is consistent with the emergence of the van Hove singularity, i.e., sharp peak ∇, in the optical conductivity spectra of the superlattices (Figure 3b). The excellent agreement of these 1D characters with the experimentally obtained optical conductivity spectra verifies the successful electronic confinement of our $(Sr_2IrO_4)_m/(LaSrGaO_4)_5$ stripe-structures.

This approach of creating 1D quantum-stripe systems provides an avenue for exploring emergent phenomena of low-dimensional physics. For instance, superconducting 1D nanostripes can be created by using an a-axis oriented superlattice of the layered cuprates such as $(La,Sr)_2CuO_4$. Although metallic ground states in true 1D materials are hard to stabilize due to structural instabilities such as the Peierls transition, the striped structures can be used to discover new phase transitions by tuning the system's dimensionality from two to one dimension(s).[28] Another intriguing feature of low dimensional systems is fractionalization of spin and charge degrees of freedom (e.g., spinons and excitons). Such excitonic effects are expected to be enhanced due to their spatial decoupling in 1D systems.

In summary, we have shown a generalizable superlattice approach of a continuous dimensional control between two dimensional (2D) layered oxides and 1D quantum stripes. We demonstrated its successful application on the highly correlated, 2D Sr_2IrO_4. In our superlattice structures, we have observed the optical transitions of electrons between neighboring Ir atoms to be confined to the 1D IrO_2 stripe direction, which emulates ideal 1D behavior. Spin and orbital excitations observed in resonant inelastic X-ray scattering also suggest enhanced spin exchange interactions and confined orbital excitations in the 1D IrO_2 stripes as compared to 2D Sr_2IrO_4. This 1D superlattice method can be readily adopted for unveiling 1D phenomena in a variety of 2D materials.

COMMUNICATION

[1] J. M. Luttinger, *J. Math. Phys.* **1963**, *4*, 1154.

[2] S. Dong, R. Yu, J. M. Liu, E. Dagotto, *Phys. Rev. Lett.* **2009**, *103*, 107204.

[3] H. A. Mook, P. C. Dai, F. Dogan, R. D. Hunt, *Nature* **2000**, *404*, 729.

[4] S. A. Kivelson, I. P. Bindloss, E. Fradkin, V. Oganesyan, J. M. Tranquada, A. Kapitulnik, C. Howald, *Rev. Mod. Phys.* **2003**, *75*, 1201.

[5] D. N. Sheng, Z. Y. Weng, L. Sheng, F. D. M. Haldane, *Phys. Rev. Lett.* **2006**, *97*, 036808.

[6] L. Fu, C. L. Kane, E. J. Mele, *Phys. Rev. Lett.* **2007**, *98*, 106803.

[7] D. Hsieh, D. Qian, L. Wray, Y. Xia, Y. S. Hor, R. J. Cava, M. Z. Hasan, *Nature* **2008**, *452*, 970.

[8] Y. L. Chen, J. G. Analytis, J. H. Chu, Z. K. Liu, S. K. Mo, X. L. Qi, H. J. Zhang, D. H. Lu, X. Dai, Z. Fang, S. C. Zhang, I. R. Fisher, Z. Hussain, Z. X. Shen, *Science* **2009**, *325*, 178.

[9] M. Imada, A. Fujimori, Y. Tokura, *Rev. Mod. Phys.* **1998**, *70*, 1039.

[10] Y. N. Xia, P. D. Yang, Y. G. Sun, Y. Y. Wu, B. Mayers, B. Gates, Y. D. Yin, F. Kim, Y. Q. Yan, *Adv. Mater.* **2003**, *15*, 353.

[11] C. Kim, A. Y. Matsuura, Z. X. Shen, N. Motoyama, H. Eisaki, S. Uchida, T. Tohyama, S. Maekawa, *Phys. Rev. Lett.* **1996**, *77*, 4054.

[12] E. Dagotto, T. M. Rice, *Science* **1996**, *271*, 618.

[13] J. Nichols, O. B. Korneta, J. Terzic, L. E. De Long, G. Cao, J. W. Brill, S. S. A. Seo, *Appl. Phys. Lett.* **2013**, *103*, 131910.

[14] S. Madhavan, D. G. Schlom, A. Dabkowski, H. A. Dabkowska, Y. Liu, *Appl. Phys. Lett.* **1996**, *68*, 559.

[15] J. Matsuno, Y. Okimoto, M. Kawasaki, Y. Tokura, *Phys. Rev. Lett.* **2005**, *95*, 176404.

[16] B. J. Kim, H. Jin, S. J. Moon, J. Y. Kim, B. G. Park, C. S. Leem, J. Yu, T. W. Noh, C. Kim, S. J. Oh, J. H. Park, V. Durairaj, G. Cao, E. Rotenberg, *Phys. Rev. Lett.* **2008**, *101*, 076402.

[17] B. J. Kim, H. Ohsumi, T. Komesu, S. Sakai, T. Morita, H. Takagi, T. Arima, *Science* **2009**, *323*, 1329.

[18] S. J. Moon, H. Jin, K. W. Kim, W. S. Choi, Y. S. Lee, J. Yu, G. Cao, A. Sumi, H. Funakubo, C. Bernhard, T. W. Noh, *Phys. Rev. Lett.* **2008**, *101*, 226402.

[19] J. H. Gruenewald, J. Nichols, J. Terzic, G. Cao, J. W. Brill, S. S. A. Seo, *J. Mater. Res.* **2014**, *29*, 2491.

[20] J. Kim, M. Daghofer, A. H. Said, T. Gog, J. van den Brink, G. Khaliullin, B. J. Kim, *Nat. Commun.* **2014**, *5*, 4453.

[21] B. H. Kim, G. Khaliullin, B. I. Min, *Phys. Rev. Lett.* **2012**, *109*, 167205.

[22] Y. K. Kim, N. H. Sung, J. D. Denlinger, B. J. Kim, *Nat. Phys.* **2016**, *12*, 37.

[23] F. Wang, T. Senthil, *Phys. Rev. Lett.* **2011**, *106*, 136402.

[24] J. H. Gruenewald, J. Nichols, S. S. A. Seo, *Rev. Sci. Instrum.* **2013**, *84*, 043902.

[25] S. J. Moon, H. Jin, W. S. Choi, J. S. Lee, S. S. A. Seo, J. Yu, G. Cao, T. W. Noh, Y. S. Lee, *Phys. Rev. B* **2009**, *80*, 195110.

[26] C. H. Sohn, M.-C. Lee, H. J. Park, K. J. Noh, H. K. Yoo, S. J. Moon, K. W. Kim, T. F. Qi, G. Cao, D.-Y. Cho, T. W. Noh, *Phys. Rev. B* **2014**, *90*, 041105.

[27] L. Van Hove, *Phys. Rev.* **1953**, *89*, 1189.

[28] E. R. Gagliano, C. R. Proetto, C. A. Balseiro, *Phys. Rev. B* **1987**, *36*, 2257.